

Theory of activated rate processes for arbitrary frequency dependent friction: solution of the turnover problem

Eli Pollak, Hermann Grabert, Peter Hänggi

Angaben zur Veröffentlichung / Publication details:

Pollak, Eli, Hermann Grabert, and Peter Hänggi. 1989. "Theory of activated rate processes for arbitrary frequency dependent friction: solution of the turnover problem." *The Journal of Chemical Physics* 91 (7): 4073–87. <https://doi.org/10.1063/1.456837>.



RESEARCH ARTICLE | OCTOBER 01 1989

Theory of activated rate processes for arbitrary frequency dependent friction: Solution of the turnover problem

Eli Pollak; Hermann Grabert; Peter Hänggi



J. Chem. Phys. 91, 4073–4087 (1989)

<https://doi.org/10.1063/1.456837>



25 September 2024 14:46:22



Nanotechnology &
Materials Science



Optics &
Photonics



Impedance
Analysis



Scanning Probe
Microscopy



Sensors



Failure Analysis &
Semiconductors



Unlock the Full Spectrum.
From DC to 8.5 GHz.

Your Application. Measured.

Find out more



Theory of activated rate processes for arbitrary frequency dependent friction: Solution of the turnover problem

Eli Pollak

Chemical Physics Department, The Weizmann Institute of Science, 76100 Rehovot, Israel

Hermann Grabert

Fachbereich Physik, Universität-GHS Essen, D-4300 Essen, Federal Republic of Germany

Peter Hänggi

Lehrstuhl für Theoretische Physik, Universität Augsburg, D-8900 Augsburg, Federal Republic of Germany

(Received 8 March 1989; accepted 8 June 1989)

An analytical theory is formulated for the thermal (classical mechanical) rate of escape from a metastable state coupled to a dissipative thermal environment. The working expressions are given solely in terms of the quantities entering the generalized Langevin equation for the particle dynamics. The theory covers the whole range of damping strength and is applicable to an arbitrary memory friction. This solves what is commonly known as the Kramers turnover problem. The basic idea underlying the approach is the observation that the escape dynamics is governed by the unstable normal mode coordinate—and not the particle system coordinate. An application to the case of a particle moving in a piecewise harmonic potential with an exponentially decaying memory-friction is presented. The comparison with the numerical simulation data of Straub, Borkovec, and Berne [J. Chem. Phys. **84**, 1788 (1986)] exhibits good agreement between theory and simulation.

I. INTRODUCTION

The movement of a Brownian particle in a field of force is frequently employed as a model for chemical reactions.¹⁻⁵ In particular, liquid state reactions are often described by the generalized Langevin equation (GLE)

$$M\ddot{q} + \frac{\partial V(q)}{\partial q} + M \int_0^t dt' \gamma(t-t') \dot{q}(t') = \xi(t). \quad (1.1)$$

The system coordinate q of effective mass M moves in a potential $V(q)$, experiences a friction kernel $\gamma(t)$ and a random force $\xi(t)$, that originate from the thermal motion of the liquid. The force $\xi(t)$ is Gaussian and satisfies the second fluctuation dissipation theorem

$$\langle \xi(t) \xi(0) \rangle = Mk_B T \gamma(t). \quad (1.2)$$

Kramers¹ treated the problem in the Markovian limit, i.e., $\gamma(t) = 2\gamma\delta(t)$, where γ is the static friction usually taken to be proportional to the viscosity of the fluid. The potential $V(q)$ is assumed to have a well with frequency ω_0 , separated from the continuum by a barrier whose height is V^\ddagger . Kramers was interested in the escape rate Γ of the particle from the well. His solution was based on the analysis of two parameter regimes. When the static friction is very weak, the rate is limited by an energy diffusion process for which Kramers showed that $\Gamma_{ED} \propto \gamma$. When the static friction is very strong, the rate is limited by spatial diffusion and it decreases as $\Gamma_{SD} \propto 1/\gamma$. As noted by Kramers, these two limiting behaviors imply a maximal rate at some γ , intermediate between the two limits. However, Kramers did not derive a single theory for the whole range of friction γ . This is the Kramers turnover problem for which an explicit solution will be presented in this paper.

Many attempts have been made to provide a single func-

tion which would bridge between both limits.^{6,7} Perhaps the simplest suggestion is the ad hoc formula⁷

$$\frac{1}{\Gamma} = \frac{1}{\Gamma_{ED}} + \frac{1}{\Gamma_{SD}} \quad (1.3)$$

Other procedures have been studied,^{8,9} however, in all of them there is always an element of arbitrariness. Even the latest beautiful theory developed by Melnikov and Meshkov⁹ uses an ad hoc multiplicative factor^{6,9} to assure that their theory reduces to the correct spatial diffusion limit.

There has been considerable interest in extending Kramers' work to the case of frequency dependent damping. In the region of moderate-to-large damping, Grote and Hynes¹⁰ and Hänggi and Mojtabai¹¹ found that the rate constants can often be much larger than one would obtain from the Kramers theory. Memory effects were also found to modify the rate constants in the limit of weak damping where the energy diffusion mechanism is the rate limiting process.¹² Based on these theories the same⁷ *ad hoc*, but useful connection formulas were proposed to obtain rate constants in the non-Markovian case for the entire range of friction parameters.

The various rate theories for frequency dependent damping were tested numerically over a large range of parameters by Straub, Borkovec, and Berne (SBB).¹³ Their work, using an exponential friction kernel, revealed striking (order of magnitude) deficiencies in the predictions based on existing theories for non-Markovian rate processes. Their results presented a twofold challenge. (i) Previous theories were not able to predict correctly the rate in the SBB limit of large damping (whose precise definition is given in Sec. IV below). (b) SBB computed the rates from weak to large

damping and observed a turnover which was not explained by existing theories.

The work of SBB stimulated quite a few theoretical papers. Hänggi³ realized that for their strong damping limit the bath correlation time is long, leading to an energy diffusion controlled limit.^{3,14,15} A quantitative approach containing some arbitrary assumptions, based on an extension of the spatial diffusion limit is given in Ref. 16 and criticized in Ref. 4. An insightful solution for the SBB strong damping limit which contains no adjustable parameters was obtained only recently by Talkner and Braun,¹⁷ thus answering the first challenge. However their work is restricted to exponential memory friction and it leaves the first challenge unanswered for an arbitrary friction kernel. The second challenge has remained completely open.

This paper will answer both challenges. In Fig. 1 we compare the results of our theory with the numerical results obtained from the SBB simulation. The theoretical results are found without the use of any adjustable parameters or *ad hoc* procedures. The theory we use, reported recently by

Grabert,¹⁸ is based on a normal mode approach to dissipative dynamics. In a recent series of papers, Pollak and co-workers¹⁹⁻²¹ have shown that much of the dissipative dynamics of GLE's can be vastly simplified using two steps. First, as shown by Zwanzig,²² one transforms, the GLE to a Hamiltonian where the system is linearly coupled to a harmonic bath. The second step is a transformation of the coordinates of the Hamiltonian to normal modes. If this is done at a barrier, one may identify uniquely the unstable normal mode. At energies close to the barrier height, the normal mode dynamics are virtually exact. This implies that a multidimensional transition state theory (TST) using the normal mode coordinates should be useful. Pollak has demonstrated the equivalence of the spatial diffusion limited rate with multidimensional TST.^{19(a)}

The key to the present theory is the observation that the unstable normal mode decouples from the other modes in the close vicinity of the barrier. This enables a formulation of a one degree of freedom stochastic process for the energy in the unstable normal mode. Using this formulation we derive an expression for the energy loss in the unstable normal mode. From the energy loss one immediately obtains the rate, the final expression is very similar to the rate expression obtained recently by Melnikov and Meshkov.⁹ We stress two crucial differences. Our theory deals with the *unstable normal mode energy* and not the energy along the physical coordinate as in Ref. 9. Secondly the present theory is formulated for arbitrary memory friction. The present theory is in practice identical to that of Melnikov and Meshkov only in the weak damping limit, it goes smoothly (without *any ad hoc* assumptions) to the correct spatial diffusion limit, which we will refer to henceforth as the multidimensional TST limit, for strong Ohmic damping.

In Sec. II we review the normal mode transformation, providing explicit continuum limit formulas for all normal mode parameters needed for the theory. In Sec. III we develop the turnover theory showing that it reduces to the correct limits, i.e., the energy diffusion or the multidimensional TST limits. The SBB system is analyzed in detail in Sec. IV. Extensions and limitations of the turnover theory are discussed in Sec. V.

II. NORMAL MODE ANALYSIS

Zwanzig²² showed that the classical mechanical stochastic process [Eqs. (1.1) and (1.2)] can be derived from the Hamiltonian function

$$H = \frac{p_q^2}{2M} + V(q) + \sum_{i=1}^N \left[\frac{p_i^2}{2m_i} + \frac{1}{2} m_i \left(\omega_i x_i - \frac{c_i}{m_i \omega_i} q \right)^2 \right] \quad (2.1)$$

where (x_i, p_i) are the coordinates and conjugate momenta of the i th bath oscillator with mass m_i and frequency ω_i . The coefficient c_i couples the i th bath oscillator to the system coordinate q . The bath parameters are defined by the friction kernel. One finds that the equation of motion for the system coordinate q is identical to the GLE [Eq. (1.1)] provided that

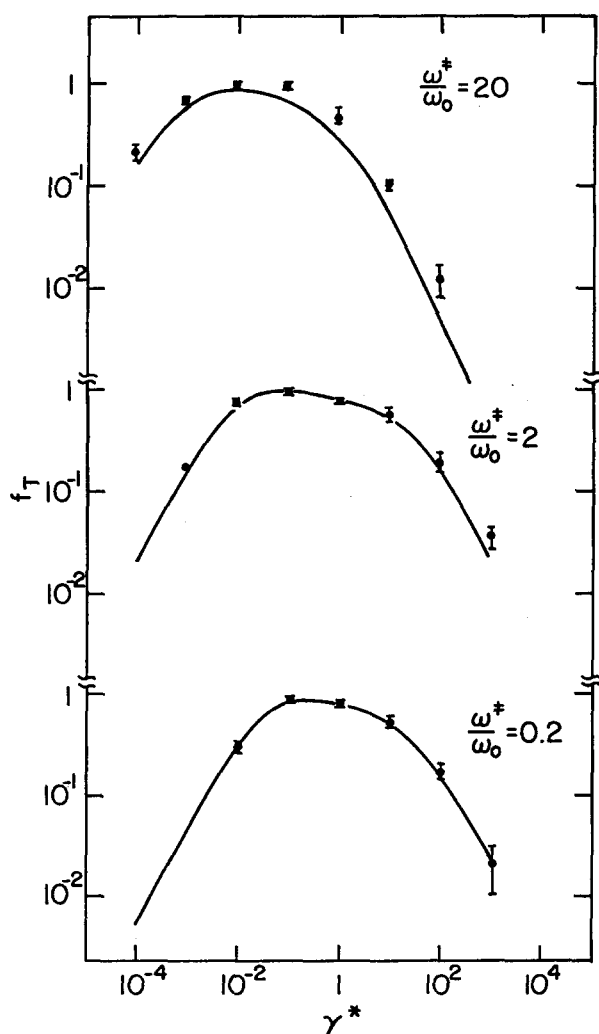


FIG. 1. Energy diffusion limited turnover. Comparison of the numerical results of SBB for a single well potential (filled circles with error bars) with the theory presented in this paper. For further details see Table I and Sec. IV B.

$$\gamma(t) = \frac{1}{M} \sum_{i=1}^N \frac{c_i^2}{m_i \omega_i^2} \cos(\omega_i t). \quad (2.2)$$

Alternatively, one can relate the bath parameters to the spectral density $J(\omega)$ through the relation

$$J(\omega) = \frac{\pi}{2M} \sum_{i=1}^N \frac{c_i^2}{m_i \omega_i} \delta(\omega - \omega_i). \quad (2.3)$$

From Eqs. (2.2), (2.3) one finds that the spectral density and the friction kernel are related by

$$J(\omega) = \omega \int_0^\infty dt \gamma(t) \cos(\omega t). \quad (2.4)$$

In recent work,¹⁹⁻²¹ we have found that the dynamics of the GLE may be simplified considerably through a normal mode transformation (whose details are given in Ref. 20) of the system and bath coordinates. We assume, that at $q = 0$, the potential $V(q)$ has a barrier, with height V^\ddagger such that a harmonic expansion around $q = 0$ leads to

$$V(q) = V^\ddagger - \frac{1}{2} M \omega^\ddagger{}^2 q^2, \quad (2.5)$$

where $\omega^\ddagger > 0$ is the unstable frequency of the barrier. The full Hamiltonian may be decomposed into a harmonic part (H_0) and a nonlinear contribution $V_1(q)$ such that

$$H = H_0 + V_1(q) \quad (2.6)$$

and

$$H_0 = \frac{p_q^2}{2M} + V^\ddagger - \frac{1}{2} M \omega^\ddagger{}^2 q^2 + \sum_{i=1}^N \left[\frac{p_i^2}{2m_i} + \frac{1}{2} m_i \left(\omega_i x_i - \frac{c_i}{m_i \omega_i} q \right)^2 \right]. \quad (2.7)$$

By construction, H_0 is a quadratic Hamiltonian which may be diagonalized. Introducing the mass weighted coordinates

$$q' = \sqrt{M} q, \quad x'_i = \sqrt{m_i} x_i \quad (2.8)$$

one finds that H_0 may be written as

$$H_0 = \frac{1}{2} \dot{\rho}^2 + V^\ddagger - \frac{1}{2} \lambda^\ddagger{}^2 \rho^2 + \sum_{i=1}^N \frac{1}{2} (\dot{y}_i^2 + \lambda_i^2 y_i^2). \quad (2.9)$$

Here, ρ denotes the unstable normal mode with frequency λ^\ddagger , y_i are the stable bath modes with frequency λ_i . The normal mode frequencies are related to the original frequencies and coupling coefficients through the relations²⁰

$$\lambda^\ddagger{}^2 = \omega^\ddagger{}^2 / \left\{ \left[\frac{1}{M} \sum_{j=1}^N \frac{c_j^2}{m_j \omega_j^2 (\omega_j^2 + \lambda^\ddagger{}^2)} \right] + 1 \right\}, \quad (2.10)$$

$$\lambda_i^2 = \omega_i^2 / \left\{ \left[\frac{1}{M} \sum_{j=1}^N \frac{c_j^2}{m_j \omega_j^2 (\lambda_i^2 - \omega_j^2)} \right] - 1 \right\}. \quad (2.11)$$

By explicit evaluation of the determinant of the force constant matrix it is also possible to prove the identity¹⁹

$$\lambda^\ddagger \prod_{i=1}^N \lambda_i = \omega^\ddagger \prod_{i=1}^N \omega_i. \quad (2.12)$$

The normal mode coordinates are just an orthogonal transformation of the original (mass weighted) coordinates. Denoting the transformation matrix as U one can express the

system coordinate q in terms of the normal mode coordinates as:

$$q' = u_{00} \rho + \sum_{i=1}^N u_{i0} y_i, \quad (2.13)$$

where the matrix elements are given by²⁰

$$u_{00} = \left[1 + \frac{1}{M} \sum_{i=1}^N \frac{c_i^2}{m_i (\lambda^\ddagger{}^2 + \omega_i^2)^2} \right]^{-1/2}, \quad (2.14)$$

$$u_{i0} = \left[1 + \frac{1}{M} \sum_{j=1}^N \frac{c_j^2}{m_j (\lambda_j^2 - \omega_i^2)^2} \right]^{-1/2}, \quad (2.15)$$

One of the important observations, which makes the normal mode transformation so useful, is that the unstable mode frequency λ^\ddagger and the matrix element u_{00} that projects onto the normal mode, may be expressed in terms of the spectral density or equivalently the friction kernel.^{19,21} Using the relation (2.3) one finds that

$$\lambda^\ddagger{}^2 = \omega^\ddagger{}^2 \left[1 + \frac{2}{\pi} \int_0^\infty d\omega \frac{J(\omega)}{\omega} \cdot \frac{1}{(\omega^2 + \lambda^\ddagger{}^2)} \right]^{-1} \quad (2.16)$$

From Eq. (2.4) one can show that the Laplace transform of the friction kernel may be written as

$$\hat{\gamma}(s) = \frac{2}{\pi} \int_0^\infty d\omega \frac{J(\omega)}{\omega} \cdot \frac{s}{(\omega^2 + s^2)}, \quad (2.17)$$

which combines with Eq. (2.16) to give the Grote-Hynes relation¹⁰ for the unique, positive valued, renormalized barrier frequency

$$\lambda^\ddagger{}^2 = \frac{\omega^\ddagger{}^2}{1 + \hat{\gamma}(\lambda^\ddagger)/\lambda^\ddagger}. \quad (2.18)$$

Since $J(\omega) \geq 0$ [implying $\hat{\gamma}(\lambda^\ddagger) > 0$] the effective barrier frequency λ^\ddagger is always smaller than the bare barrier frequency ω^\ddagger .

Similarly, using Eq. (2.3) one finds for the matrix element u_{00} ²¹:

$$u_{00}^2 = \left[1 + \frac{2}{\pi} \int_0^\infty d\omega \frac{J(\omega) \cdot \omega}{(\omega^2 + \lambda^\ddagger{}^2)^2} \right]^{-1}. \quad (2.19)$$

Defining a "perturbation parameter" ϵ as

$$\epsilon = \frac{1}{u_{00}^2} - 1 = \sum_{i=1}^N \left(\frac{u_{i0}}{u_{00}} \right)^2, \quad (2.20)$$

using Eqs. (2.17) and (2.19), gives the interesting relation

$$\epsilon = \frac{2}{\pi} \int_0^\infty d\omega \frac{J(\omega) \cdot \omega}{(\omega^2 + \lambda^\ddagger{}^2)^2} = \frac{1}{2} \left[\frac{\hat{\gamma}(\lambda^\ddagger)}{\lambda^\ddagger} + \frac{\partial \hat{\gamma}(\lambda^\ddagger)}{\partial \lambda^\ddagger} \right]. \quad (2.21)$$

Clearly, in the weak damping limit, ϵ is small, but we shall see in the next sections that for memory friction, ϵ can remain a small parameter also when seemingly the damping parameter $[\hat{\gamma}(0)]$ is very large.

In anticipation of the theory developed in the next section we provide one additional crucial identity relating the normal mode transformation to the Laplace transform of the

friction kernel. We will see in the next section that the function

$$K(t) = \sum_{i=1}^N \frac{u_{i0}^2}{u_{00}^2} \cos(\lambda_i t) \quad (2.22)$$

is needed to determine the energy loss of the system due to interaction with the thermal bath. In Ref. 21 it is shown that the Laplace transform $\hat{K}(s)$ of this function may be written as

$$\begin{aligned} \hat{K}(s) &= \sum_{i=1}^N \frac{u_{i0}^2}{u_{00}^2} \frac{s}{(s^2 + \lambda_i^2)} \\ &= \frac{1}{u_{00}^2} \cdot \frac{s}{(s^2 + s\hat{\gamma}(s) - \omega^{\neq 2})} - \frac{s}{(s^2 - \lambda^{\neq 2})}. \end{aligned} \quad (2.23)$$

The first expression on the right-hand side is obtained by the direct Laplace transform of Eq. (2.22), the second expression is less trivial and is obtained by inversion of the force constant matrix [cf. Appendix A of Ref. 21(a)]. An alternative derivation is given in Appendix A.

To summarize, the properties of the normal mode transformation provide three basic relations between the normal mode coordinates and their continuum limit. These are the Grote Hynes relation—Eq. (2.18), the projection relation—Eqs. (2.19)–(2.21), and the relation of the Laplace transform of $K(t)$ with the memory friction, $\hat{\gamma}(s)$, Eq. (2.23). With these tools we are able to express the turnover theory presented in the next section in terms of the system parameters and the memory friction.

III. THE TURNOVER THEORY

A. The multidimensional TST limit

The general problem we consider is that of a particle trapped in a well (with harmonic frequency ω_0), separated from the continuum by a barrier, cf. Fig. 2. Escape is possible only by a crossing of the barrier. At the barrier, the total energy becomes the sum of the normal mode energies. Let us denote by E_i the energy in the stable modes y_i and by E the remaining energy in the unstable mode ρ . Since the normal modes are not coupled, the probability to cross the barrier region depends on the energy E only. For $E > V^{\neq}$ the particle leaves the well while for $E < V^{\neq}$ the ρ -component of the trajectory goes through a turning point and the particle returns to the well.

Following Kramers¹ we now imagine injecting particles at a constant rate near the bottom of the well and removing them from the continuum (or the adjacent well). The system will then approach a steady-state probability with a constant flux across the barrier. Let W be this steady-state probability normalized to one particle in the well. We assume here and in the sequel that the barrier height V^{\neq} is much larger than $k_B T$. Then, apart from corrections exponentially small in $V^{\neq}/k_B T$, the probability W will concentrate near the bottom of the well and it can be replaced by a Boltzmann distribution there. As a first approximation we shall assume that this Boltzmann distribution remains valid even near the top of the barrier. Clearly, this assumption is reasonable only

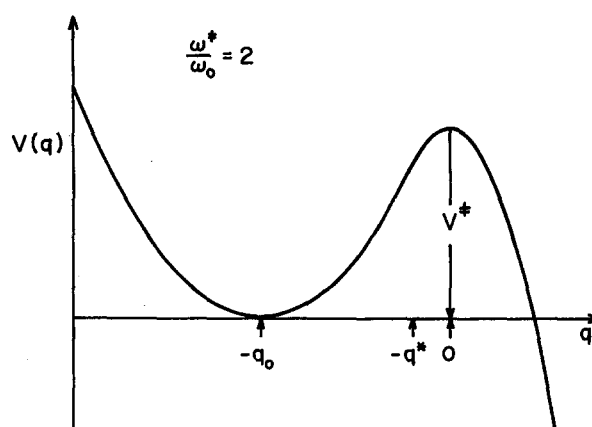


FIG. 2. Schematic diagram of the generic system potential energy for the escape of a trapped particle. The diagram is shown for the piecewise continuous harmonic oscillator potential used in the SBB simulation (cf. Sec. IV A).

under certain conditions to be specified below.³ Since the Hamiltonian decomposes in the barrier region according to (2.9), the Boltzmann distribution factorizes into

$$\begin{aligned} W_{\text{eq}} &= \frac{1}{Z} \left[\prod_{i=1}^N \exp \left[-\beta \left(\frac{1}{2} \dot{y}_i^2 + \frac{1}{2} \lambda_i^2 y_i^2 \right) \right] \right] \\ &\quad \times \exp \left[-\beta \left(\frac{1}{2} \dot{\rho}^2 + V^{\neq} - \frac{1}{2} \lambda^{\neq 2} \rho^2 \right) \right], \end{aligned} \quad (3.1)$$

where $\beta = 1/k_B T$ and where Z is a normalization factor. For high barriers the contributions to Z come from the well region only. There we may introduce another normal mode system. The calculation will not be given here since it is very similar to the normal mode analysis presented in the preceding section. Normalizing the probability to one particle in the well we find (using an identity similar to Eq. (2.12) for the normal modes at the well)

$$Z = \frac{\beta \omega_0}{2\pi} \prod_{i=1}^N \frac{\beta \omega_i}{2\pi}. \quad (3.2)$$

Integrating (3.1) over the stable mode coordinates, we obtain by means of (2.12) for the equilibrium distribution of the unstable mode coordinates

$$\begin{aligned} W_{\text{eq}}(\dot{\rho}, \rho) &= \frac{\beta \omega_0}{2\pi} \frac{\lambda^{\neq}}{\omega^{\neq}} \\ &\quad \times \exp \left[-\beta \left(\frac{1}{2} \dot{\rho}^2 + V^{\neq} - \frac{1}{2} \lambda^{\neq 2} \rho^2 \right) \right]. \end{aligned} \quad (3.3)$$

When the energy in the unstable normal mode

$$E = \frac{1}{2} \dot{\rho}^2 + V^{\neq} - \frac{1}{2} \lambda^{\neq 2} \rho^2 \quad (3.4)$$

is smaller than V^{\neq} , the trajectory will reach a turning point where $\dot{\rho} = 0$. As pointed out by Grabert,¹⁸ the crucial quantity needed for an estimate of the decay rate, is the distribution of energy in the unstable normal mode. For $E < V^{\neq}$ let $f(E) dE dt$ denote the probability to find the system within the time interval dt , with a mode energy between E and $E + dE$ at a turning point of the ρ mode. From Eq. (3.3) it is seen that a

thermal distribution near the barrier yields for this probability

$$f_{\text{eq}}(E) = \frac{\beta \omega_0}{2\pi} \frac{\lambda^\#}{\omega^\#} \exp(-\beta E). \quad (3.5)$$

Near a turning point ($\rho = \rho_T, \dot{\rho} = 0$) one has $dE = -\lambda^\# \rho_T d\rho$ and $d\rho = \rho_T \lambda^\# dt$ so that

$$|dE dt| = |d\rho d\dot{\rho}| \quad (3.6)$$

and the Jacobian of the transformation leading to Eq. (3.5) equals 1.

For $E > V^\#$ the system crosses the barrier. Now we denote by $f(E)dE dt$ the probability to find the system at the barrier ($\rho = 0$), within the time interval dt and with a normal mode energy between E and $E + dE$. A similar reasoning as above shows that the thermal distribution near the barrier (3.3) leads again to Eq. (3.5). This means that Eq. (3.5) gives the likelihood, at thermal equilibrium, to find the system at a turning point or at the barrier depending on whether E is smaller or larger than the barrier energy.

In terms of the steady state probability $f(E)$, the rate of transitions out of the well can be written

$$\Gamma = \int_{V^\#}^{\infty} dE f(E) \quad (3.7)$$

since all particles reaching the barrier with $E > V^\#$ escape with probability 1. As discussed in a previous paper,¹⁸ the recrossing problem does not occur in the normal mode representation. It is this crucial observation which enables the extension of the Melnikov and Meshkov approach⁹ to parameter regimes outside of the weak damping limit. Due to the interaction with the bath modes, the system coordinate q behaves stochastically and it may cross the point $q = 0$ several times during an escape event. These fluctuations are absent in the ρ -coordinate since it decouples from the other modes and hence moves smoothly near the barrier. It should be noted that the normal mode energy E differs from the mechanical energy $E_q = \frac{1}{2}M\dot{q}^2 + V(q)$ of the particle. The two energies are equal only in the absence of damping.

The rate formula (3.7) is formally exact. Approximations enter because the nonequilibrium probability $f(E)$ is not known exactly. In the following subsections we shall calculate $f(E)$ for systems with high barriers. Before doing so let us discuss a simple approximation. Replacing $f(E)$ by the equilibrium probability $f_{\text{eq}}(E)$, Eq. (3.5), we obtain from (3.7)

$$\Gamma = \frac{\omega_0}{2\pi} \frac{\lambda^\#}{\omega^\#} \exp(-\beta V^\#) \quad (3.8)$$

which is just the result obtained by Grote and Hynes¹⁰ and Hänggi and Mojtabai¹¹ along quite different lines. As discussed in a previous paper,¹⁹ the normal mode analysis shows that Eq. (3.8) is just the multidimensional transition state theory result. It differs from the simple one-dimensional transition state theory rate by the factor $\lambda^\#/\omega^\#$ describing a reduction of the rate caused by the damping of the reaction coordinate.

The rate formula (3.8) is based on the assumption of a thermal distribution of the energy E in the unstable normal mode near the barrier. This will only be the case when the ρ

mode and the stable modes are coupled sufficiently strongly in the well region so that the mode energy E is thermalized whenever the system returns to the metastable well. In the general case, the energy exchange between the unstable and the stable modes has to be studied explicitly, a problem we shall address in the following subsection.

B. Energy loss and energy fluctuations

When the system fluctuates to the barrier region and the energy E in the unstable normal mode is below the barrier energy $V^\#$, the particle returns to the well where all modes are coupled by the potential $V_1(q)$ [cf. Eq. (2.6)]. For $E' < V^\#$ let us introduce¹⁸ the conditional probability $P(E|E')dE$ that a system leaving the barrier region with energy E' in the ρ mode returns to the barrier with an energy between E and $E + dE$. This probability satisfies the condition of detailed balance

$$P(E|E') \exp(-\beta E') = P(E'|E) \exp(-\beta E) \quad (3.9)$$

and it tends to thermalize the energy in the unstable normal modes. Now, in the steady state under consideration, particles are injected into the well and removed beyond the barrier. Because of the steady flux from the well outwards, the distribution $f(E)$ introduced in the preceding section may deviate from its equilibrium form $f_{\text{eq}}(E)$, Eq. (3.5). In general, $f(E)$ has to be calculated from the steady state condition

$$f(E) = \int_0^{V^\#} dE' P(E|E') f(E'). \quad (3.10)$$

For energies a few times $k_B T$ below the barrier energy, the probability $f(E)$ will approach $f_{\text{eq}}(E)$ since $P(E|E')$ satisfies the detailed balance condition (III.9). Hence, the conditional probability $P(E|E')$ is needed only for energies near the barrier energy. Furthermore, when the modes are coupled strongly in the well region, a large fraction of the energy E' will usually be absorbed by the stable modes during a traversal of the well. As a function of E the conditional probability $P(E|E')$ will then have only a small Boltzmann tail for energies near $E = V^\#$. Under these conditions, Eq. (3.10) is very accurately solved by $f_{\text{eq}}(E)$ and deviations from the multidimensional TST theory result are not important. Hence, we are in the favorable situation that the conditional probability $P(E|E')$ has to be determined only for the case of weak coupling between the unstable and the stable modes in the well region.

Using Eqs. (2.6), (2.9), and (2.13) we readily obtain for the equations of motion in the normal mode basis

$$\ddot{\rho} - \lambda^\# \rho = -u_{00} V_1' \left(u_{00} \rho + \sum_{i=1}^N u_{i0} y_i \right) \quad (3.11)$$

and

$$\ddot{y}_i + \lambda_i^2 y_i = -u_{i0} V_1' \left(u_{00} \rho + \sum_{i=1}^N u_{i0} y_i \right), \quad (3.12)$$

where

$$V_1'(x) \equiv \frac{1}{\sqrt{M}} \frac{dV_1(x/\sqrt{M})}{dx}.$$

The coupling between the unstable and the stable modes in the well region arises through the coefficients

$$g_i = u_{i0}/u_{00} \quad (3.13)$$

and the weak coupling limit may be characterized by [cf. Eq. 2.20)]

$$\epsilon = \sum_{i=1}^N g_i^2 \ll 1. \quad (3.14)$$

It should be stressed (as is also demonstrated explicitly in Sec. IV) that this definition of the weak coupling limit is much more general than the usual definition which corresponds to weak damping. The static friction $[\hat{\gamma}(0)]$ may be large in magnitude and still $\epsilon \ll 1$, leading to deviations from the multidimensional TST limit, in agreement with Hänggi's arguments.³

In order to calculate $P(E|E')$ let us assume that at $t = t_0$ the ρ mode is in the barrier region at the turning point corresponding to the initial mode energy E' . To find the probability that the system returns to the barrier region with energy E we solve the exact equations of motion (3.11) and (3.12) to first order in the coupling coefficients g_i . For the unstable mode the zero order equation of motion is

$$\ddot{\rho} - \lambda^2 \rho = -u_{00} V_1'(u_{00} \rho). \quad (3.15)$$

For zero damping this reduces to the equation of motion of the system coordinate q . However, if the damping is non-zero, the ρ mode for zero coupling is governed by an effective potential which may substantially differ from the original potential $V(q)$. Given the initial conditions (turning point and energy) it is straightforward to solve the unperturbed ρ -mode equation of motion (3.15) and thus the time t_p needed to return to the turning point.

The first order equations of motion for the stable modes then read

$$\ddot{y}_i = -\lambda_i^2 y_i + g_i F \quad (3.16)$$

with the force F given by

$$F = -u_{00} V_1'(u_{00} \rho). \quad (3.17)$$

In Eq. (3.17), one inserts the solution for the zero order ρ motion, Eq. (3.15). Thus, to first order, the stable mode equation of motion is that of a forced harmonic oscillator whose solution is well known:

$$y_i(t) = y_i(0) \cos(\lambda_i t) + \dot{y}_i(0) \frac{\sin(\lambda_i t)}{\lambda_i} + \int_0^t dt' \frac{\sin[\lambda_i(t-t')]}{\lambda_i} g_i F(t'). \quad (3.18)$$

The positions $y_i(0)$ and velocities $\dot{y}_i(0)$ of the stable modes are assumed to be distributed thermally, i.e.,

$$\langle y_i(0) \rangle = \langle \dot{y}_i(0) \rangle = \langle y_i(0) \dot{y}_i(0) \rangle = 0, \quad (3.19)$$

$$\lambda_i^2 \langle y_i^2(0) \rangle = \langle \dot{y}_i^2(0) \rangle = k_B T.$$

The energy in the y_i mode (which is well defined in the near vicinity of the barrier where the anharmonicity may be neglected)

$$E_i = \frac{1}{2} \dot{y}_i^2 + \frac{1}{2} \lambda_i^2 y_i^2 \quad (3.20)$$

changes during the transversal of the ρ -mode over the time t_p according to

$$E_i(t_p) = E_i(0) + \frac{1}{2} g_i^2 \int_0^{t_p} dt \int_0^{t_p} dt' \times \cos[\lambda_i(t-t')] F(t) F(t') + g_i \int_0^{t_p} dt [\dot{y}_i(0) \cos(\lambda_i t) - y_i(0) \lambda_i \times \sin(\lambda_i t)] F(t) \quad (3.21)$$

as can be verified from Eq. (3.18).

In principle $F(t)$, determined by the uncoupled ρ -mode equation of motion (3.16), is dependent on the initial energy E' . However, if the barrier is large ($\beta V^\ddagger \gg 1$) then variations in $E_i(t_p) - E_i(0)$ with energy will be of the order $(V^\ddagger - E')/V^\ddagger$. Since $V^\ddagger - E'$ is of order $k_B T$, the condition that the barrier is large assures that such corrections may be neglected. It suffices to evaluate $F(t)$ at the barrier energy $E' = V^\ddagger$. The unperturbed ρ mode is then the motion that starts asymptotically close to the barrier and returns asymptotically to the barrier at time $t_p \rightarrow \infty$.

With these preliminaries we are able to determine the conditional probability $P(E|E')$. Since the energy absorbed by all stable modes equals the energy loss of the unstable mode, we find¹⁸ from Eqs. (3.19) and (3.21) that the energy E in the unstable mode when the system returns to the barrier is

$$E = E' - \Delta E + \delta E, \quad (3.22)$$

where

$$\Delta E = \frac{1}{2} \sum_{i=1}^N g_i^2 \int_0^{t_p} dt \int_0^{t_p} dt' \cos[\lambda_i(t-t')] F(t) F(t') \quad (3.23)$$

is the average energy loss, and δE are Gaussian fluctuations about $\langle E \rangle = E' - \Delta E$ with

$$\langle \delta E \rangle = 0; \quad \langle \delta E^2 \rangle = 2k_B T \Delta E. \quad (3.24)$$

Hence, in the limit $\beta V^\ddagger \gg 1$, the relevant part of the distribution $P(E|E')$ takes the form¹⁸

$$P(E|E') = (4\pi k_B T \Delta E)^{-1/2} \times \exp[-(E - E' + \Delta E)^2 / 4k_B T \Delta E] \quad (3.25)$$

This conditional probability satisfies the condition of detailed balance (3.9). It should be stressed here that ΔE is a positive quantity as may be seen by inserting the identity

$$\cos[\lambda_i(t-t')] = \cos(\lambda_i t) \cos(\lambda_i t') + \sin(\lambda_i t) \sin(\lambda_i t') \quad (3.26)$$

into Eq. (3.23). This leads to the result

$$\Delta E = \frac{1}{2} \sum_{i=1}^N g_i^2 \left\{ \left[\int_0^{t_p} dt \cos(\lambda_i t) F(t) \right]^2 + \left[\int_0^{t_p} dt \sin(\lambda_i t) F(t) \right]^2 \right\} \geq 0. \quad (3.27)$$

Note also, that although the form of Eq. (3.25) is identical to Eq. (3.7) of Ref. 9, the two are fundamentally different. In

Ref. 9, E, E' denote energies along the system coordinate. Here, they denote the energy in the unstable mode. As a result, the average energy loss given by Eq. (2.23) is usually quite different from the estimate based on the weak damping diffusion equation.

The average energy loss, Eq. (3.23) may be written as [cf. Eq. (2.22)]

$$\Delta E = \frac{1}{2} \int_0^{t_p} dt \int_0^{t_p} dt' K(t-t') F(t) F(t'). \quad (3.28)$$

$K(t)$ is known in the continuum limit [Eq. (2.23)], and the ρ -mode unperturbed equation of motion [Eq. (3.15)] involves quantities such as u_{00} and $\lambda^\#$ whose continuum limit is also known. Here, continuum limit means that all functions are expressed in terms of the quantities entering the GLE, Eq. (1.1). This implies that we have obtained an explicit solution for the energy loss ΔE and the conditional probability $P(E|E')$. It is now straightforward,^{9,18} to obtain the rate, as shown in the next subsection.

It is of interest to derive a slightly different form for the energy loss expression. Integrating Eq. (3.28) by parts and observing that $F(0) = F(t_p \rightarrow \infty) = 0$ [since $F(t)$ is determined by the asymptotic orbit] we find

$$\Delta E = \frac{1}{2} \int_0^\infty dt \int_0^\infty dt' \phi(t-t') \dot{\rho}(t) \dot{\rho}(t'). \quad (3.29)$$

Here $\phi(t)$ is an effective friction kernel

$$\phi(t) = \sum_{i=1}^N \frac{g_i^2}{\lambda_i^2} (\lambda_i^2 + \lambda^{\#2})^2 \cos(\lambda_i t). \quad (3.30)$$

In the weak damping limit, one finds [cf. Eqs. (2.11), (2.15), or Ref. 19] that the transformation matrix elements are approximately

$$u_{00}^2 \approx \frac{c_i^2}{M m_i (\omega_i^2 + \omega^{\#2})^2} \quad (3.31)$$

so that in the weak damping limit $\phi(t)$ reduces to the memory friction $\gamma(t)$. This shows that in this limit, our expression for the energy loss is identical to the expression of Zwanzig,²³ see also Ref. 17. In principle, taking the Laplace transform of $\phi(t)$ and using the identity given in Eq. (2.23) one can derive a continuum expression for $\hat{\phi}(s)$, similar to Eq. (2.23). In practice, the resulting expression is less tractable than Eq. (2.23) so that we will use only Eq. (3.28).

C. The rate

We now want to calculate the reaction rate explicitly. As discussed in the beginning of this section, deviations from the multidimensional TST rate arise from deviations of the probability $f(E)$ from its equilibrium from $f_{eq}(E)$. The probability $f(E)$ has to be calculated from the steady state condition (3.10). Since the probability $P(E|E')$, Eq. (3.25), satisfies the detailed balance condition (3.9), Eq. (3.10) has a solution $f(E)$ approaching $f_{eq}(E)$ for $V^\# - E \gg k_B T$. It is convenient to make the ansatz¹⁸

$$f(E) = f_{eq}(E) \exp[\frac{1}{2} \beta (E - V^\#)] \phi[\beta (E - V^\#)]$$

which transforms (3.10) into a Wiener-Hopf equation with a symmetric kernel that can be solved by standard meth-

ods.^{9,24} Combining the solution with (3.7) the escape rate is then found to be of the form

$$\Gamma = \frac{\omega_0}{2\pi} f_T \exp(-\beta V^\#), \quad (3.32)$$

where the transmission factor f_T describes the deviations due to the friction. We have

$$f_T = \frac{\lambda^\#}{\omega^\#} \exp\left[\frac{1}{\pi} \int_{-\infty}^{+\infty} \frac{dy}{1+y^2} \ln(1 - e^{-\delta(1+y^2)^{1/4}})\right], \quad (3.33)$$

where

$$\delta = \Delta E / k_B T. \quad (3.34)$$

For $\delta \gg 1$ the transmission factor (3.33) approaches $f_T = \lambda^\# / \omega^\#$ exponentially fast. In this region $f(E)$ is very close to $f_{eq}(E)$ and the escape rate is given by the multidimensional TST result, Eq. (3.8), which is independent of the precise form of $P(E|E')$. Nonequilibrium effects in $f(E)$ are only important for δ of order 1, or smaller.

To conclude this section we summarize the conditions which are necessary for the validity of the present theory.

(a) First order perturbation approximation, $\epsilon \ll 1$.

(b) Neglect of corrections to steepest descent, $V^\# \gg k_B T$.

The first condition assures the validity of the perturbation theory estimate of the energy loss, through the perturbative solution of the normal mode equations of motion (3.11) and (3.12). Given the friction kernel $\gamma(t)$ it is easy to estimate ϵ [cf. Eq. (2.21)]. Small ϵ leads to a small energy loss so that the rate is essentially limited by the energy diffusion process. The second condition which is somewhat more tricky is needed to assure the validity of the estimate for the rate (3.33), given the energy loss. Note that $P(E|E')$ is the conditional probability for the energy with respect to the ρ mode. Thus it is not sufficient that condition *b* holds for the system coordinate q . It is necessary that the effective barrier height for the unperturbed ρ -mode [Eq. 3.15] be much larger than $k_B T$. From Eq. (3.15) it follows that the unperturbed ρ motion is governed by the Hamiltonian

$$h_\rho = \frac{1}{2} \dot{\rho}^2 + V^\# - \frac{1}{2} \lambda^{\#2} \rho^2 + V_1(u_{00} \rho / \sqrt{M}) \equiv \frac{1}{2} \dot{\rho}^2 + Q(\rho). \quad (3.35)$$

The effective potential $Q(\rho)$ will generally have a barrier height $Q^\#$ which is different from $V^\#$. Thus, the more precise statement of condition (b) is

$$k_B T \ll Q^\#. \quad (b')$$

To estimate whether this condition holds one must first estimate the continuum limit of $Q(\rho)$.

From Eq. (3.33) we already noted that nonequilibrium effects in $f(E)$ are important only for $\delta = \beta \Delta E \lesssim 1$. From condition (b') we can thus derive a third condition for validity of the theory, namely

$$\Delta E \ll Q^\#. \quad (c)$$

We will see in the application presented in the next section that in practice it is condition (c) which is crucial.

It should be stressed though that when $\epsilon \gtrsim 1$ the theory does not necessarily break down. If $\epsilon \gtrsim 1$ leads to a large

energy loss, then although the estimate of the energy loss is not accurate, the estimate for the rate remains valid. When $\beta\Delta E \gg 1$, the rate [Eq. (3.33)] is exponentially insensitive to the magnitude of $\beta\Delta E$ and leads to the multidimensional TST limit. Only in the case that $\epsilon \gg 1$ but the estimated energy loss Eq. (3.28) $\beta\Delta E \ll 1$, will the present theory provide an unreliable estimate of the rate.

Finally, we note that for $\delta \ll 1$, the transmission factor (3.33) approaches $f_T = \beta\Delta E(\lambda^\neq/\omega^\neq)$ which reduces in the weak damping limit to the well known energy diffusion estimate for the rate, i.e.,

$$\Gamma_{ED} \approx \beta\Delta E \frac{\omega_0}{2\pi} \exp(-\beta V^\neq). \quad (3.36)$$

IV. AN APPLICATION: THE SINGLE WELL SBB PROBLEM

A. The system

As described in the Introduction, the extensive numerical studies of Straub, Borkovec and Berne¹³ showed that all previous theories were not sufficient for a general understanding of activated barrier crossing rates. Here, we apply the theory developed in the previous sections to the single well SBB system. The potential to be studied is the piecewise continuous parabolic potential

$$V(q) = \begin{cases} \frac{1}{2} M\omega_0^2 (q + q_0)^2, & q < -q^* \\ V^\neq - \frac{1}{2} M\omega^\neq^2 q^2, & q \geq -q^* \end{cases}, \quad (4.1)$$

where the continuous matching of $V(q)$ and its derivative at $q = -q^*$ implies

$$q_0 = \left(1 + \frac{\omega^\neq^2}{\omega_0^2}\right) q^*, \quad V^\neq = \frac{1}{2} M\omega^\neq^2 q_0^2 \quad (4.2)$$

A plot of this potential with typical parameters is shown in Fig. 2. The nonlinear part of this potential [cf. Eq. (2.6)] has the simple form:

$$V_1(q) = \begin{cases} \frac{1}{2} M(\omega_0^2 + \omega^\neq^2) (q + q^*)^2, & q \leq -q^* \\ 0, & \text{otherwise} \end{cases}. \quad (4.3)$$

The friction kernel used by SBB is an exponential

$$\gamma(t) = \alpha^{-1} \exp(-t/\alpha\gamma) \quad (4.4)$$

which gives for the Laplace transform

$$\hat{\gamma}(s) = \frac{\gamma}{1 + s\alpha\gamma}. \quad (4.5)$$

Here $\gamma = \hat{\gamma}(0)$ is the static friction and α is essentially the inverse of the infinite frequency shear modulus of the solvent. The SBB model is thus defined in terms of the five parameters ω_0 , ω^\neq , V^\neq , α , γ .

$$Q(\rho) = \begin{cases} \frac{1}{2} \lambda_0^2 \left[\rho + \frac{\omega_0^2}{\lambda_0^2} u_{00} q_0' \right]^2 + \frac{1}{2} \omega_0^2 q_0'^2 \left(1 - \frac{\omega_0^2}{\lambda_0^2} u_{00}^2 \right), & \rho \leq -\rho^* \\ V^\neq - \frac{1}{2} \lambda^\neq^2 \rho^2, & \rho \geq -\rho^* \end{cases}, \quad (4.14)$$

where $q_0' = \sqrt{M} q_0$ and the effective well frequency λ_0 is given by

$$\lambda_0^2 = u_{00}^2 (\omega_0^2 + \omega^\neq^2) - \lambda^\neq^2. \quad (4.15)$$

The first step towards solution of the problem is to determine λ^\neq and ϵ . From Eq. (2.18) we obtain

$$(\lambda^\neq^2 - \omega^\neq^2)(1 + \alpha\gamma\lambda^\neq) + \gamma\lambda^\neq = 0. \quad (4.6)$$

This cubic equation for λ^\neq has one positive root, the Grote-Hynes frequency. In order to proceed it is convenient to introduce a dimensionless damping parameter

$$\gamma^* = \gamma/\omega^\neq \quad (4.7)$$

and another dimensionless parameter

$$\alpha^* = \alpha\omega^\neq^2 \quad (4.8)$$

characterizing the deviation of $\gamma(t)$, Eq. (4.4), from a Markovian damping kernel. For weak damping, $\gamma^* \ll 1$, we find from Eq. (4.6),

$$\frac{\lambda^\neq}{\omega^\neq} = 1 - \frac{1}{2} \gamma^* + \frac{1}{8} (1 + 4\alpha^*) \gamma^{*2} \quad (4.9)$$

while for strong damping, $\gamma^* \gg 1$, we have

$$\frac{\lambda^\neq}{\omega^\neq} = \begin{cases} \left(\frac{\alpha^* - 1}{\alpha^*} \right)^{1/2} + \frac{1}{2\alpha^*(\alpha^* - 1)} \cdot \frac{1}{\gamma^*} & \text{for } \alpha^* > 1 \\ \frac{1}{1 - \alpha^*} \cdot \frac{1}{\gamma^*} & \text{for } \alpha^* < 1 \end{cases} \quad (4.10)$$

Near $\alpha^* = 1$ the high damping limit becomes nontrivial since λ^\neq depends on the relative size of $\alpha^* - 1$ and $1/\gamma^*$. In particular, for $\alpha^* = 1$ we have in the strong damping limit

$$\frac{\lambda^\neq}{\omega^\neq} = \frac{1}{\gamma^{*1/3}} - \frac{1}{3\gamma^*}. \quad (4.11)$$

Using Eq. (2.21) we find that the perturbation parameter ϵ is

$$\epsilon = \frac{\gamma^* \omega^\neq / \lambda^\neq}{2(1 + \alpha^* \gamma^* \lambda^\neq / \omega^\neq)^2}. \quad (4.12)$$

Clearly, the weak coupling condition is satisfied for weak damping, $\gamma^* \ll 1$, but also for strong damping, $\gamma^* \gg 1$, provided $\alpha^* > 1$ [cf. Eq. (4.10)]. In both of these limits we expect to find strong deviations from the multidimensional TST rate.

The equation of motion for the uncoupled ρ mode is

$$\ddot{\rho} = \begin{cases} \lambda^\neq^2 \rho - u_{00}^2 (\omega_0^2 + \omega^\neq^2) (\rho + \rho^*), & \rho \leq -\rho^* \\ \lambda^\neq^2 \rho, & \rho \geq -\rho^* \end{cases}, \quad (4.13)$$

where $\rho^* = \sqrt{M} q^* / u_{00}$. The effective potential for the uncoupled ρ mode [cf. Eq. (3.35)] is

It follows that the effective barrier height for the uncoupled ρ -mode motion is

$$Q^\neq = V^\neq \frac{\lambda^\neq^2}{\lambda_0^2} \frac{\omega_0^2}{\omega^\neq^2}. \quad (4.16)$$

We will see in the next subsection that for various parameter ranges $Q^* \ll V^*$ so that the theory must be applied carefully.

The equations of motion for the ρ mode at the energy $E = V^*$ are easily solved. Because of the piecewise parabolic nature of the potential, the force $F(t) = 0$ as long as $\rho \geq -\rho^*$. To evaluate the energy loss we must determine $F(t)$ only in the time interval $[0, t_p]$ defined such that

$$\rho(0) = \rho(t_p) = -\rho^*, \quad (4.17)$$

$$\dot{\rho}(0) = -\dot{\rho}(t_p) = -\lambda^* \rho^*. \quad (4.18)$$

Thus t_p is the time it takes the ρ mode to traverse the well region once at the energy V^* . With these boundary conditions, the solution of Eqs. (4.13) leads to the following expression for $F(t)$:

$$F(t) = \frac{\lambda^*}{\lambda_0^2} (\lambda_0^2 + \lambda^{*2}) \rho^* \times \left[1 - \cos \lambda_0 t + \frac{\lambda_0}{\lambda^*} \sin(\lambda_0 t) \right], \quad 0 \leq t \leq t_p. \quad (4.19)$$

The traversal time t_p is determined from the equations

$$\cos(\lambda_0 t_p) = \frac{\lambda^{*2} - \lambda_0^2}{\lambda_0^2 + \lambda^{*2}}, \quad \sin(\lambda_0 t_p) = \frac{-2\lambda_0 \lambda^*}{\lambda_0^2 + \lambda^{*2}}. \quad (4.20)$$

Since $\lambda_0, \lambda^* > 0$, it is evident that $\pi \leq \lambda_0 t_p < 2\pi$.

The only element now missing for computation of the energy loss is the function $K(t)$ [Eqs. (2.22)] whose Laplace transform is known through Eqs. (2.23) and (4.5). To invert the Laplace transform we first note that the pole at the Grote-Hynes frequency λ^* of the first term in Eq. (2.23) is compensated by a corresponding pole of the second term. This cancellation occurs for arbitrary damping and follows by means of [Eq. (2.18)]. All other poles of $\tilde{K}(z)$ have negative real parts so that $K(t)$ approaches 0 for $t \rightarrow \infty$.

For the exponentially decaying memory function, Eq. (4.4), the additional poles of the first term in Eq. (2.23) are at

$$z_{\pm} = -\xi \pm \sigma, \quad (4.21)$$

where

$$\xi = \frac{1}{2} \left(\lambda^* + \frac{1}{\alpha \gamma} \right) \quad (4.22)$$

and

$$\sigma^2 = \xi^2 - \frac{\omega^{*2}}{\alpha \gamma \lambda^*}. \quad (4.23)$$

The quantity σ can be real or imaginary. The second term in Eq. (2.23) has a further pole at $z = -\lambda^*$. Calculating the residues, one readily determines the inverse Laplace transform

$$K(t) = \frac{1}{2} \exp(-\xi t) \left[(1 + 2\epsilon) \cosh(\sigma t) + \frac{(1 + 2\epsilon)\xi - \lambda^*}{\sigma} \sinh(\sigma t) \right] - \frac{1}{2} \exp(-\lambda^* t). \quad (4.24)$$

Inserting now Eqs. (4.19) and (4.24) into Eq. (3.28), one finds that the average energy loss may be written as

$$\Delta E = V^* \frac{\omega_0^2}{\omega^{*2}} \frac{\lambda^{*2} (\lambda_0^2 + \lambda^{*2})}{\lambda_0^4} \times \left\{ \frac{1}{2} (1 + 2\epsilon) [R(\xi + \sigma) + R(\xi - \sigma)] - \frac{(1 + 2\epsilon)\xi - \lambda^*}{2\sigma} \times [R(\xi + \sigma) - R(\xi - \sigma)] - R(\lambda^*) \right\}, \quad (4.25)$$

where we introduced

$$R(z) = \int_0^{t_p} dt \int_0^t dt' e^{-z(t-t')} \times \left[1 - \cos(\lambda_0 t) + \frac{\lambda_0}{\lambda^*} \sin(\lambda_0 t) \right] \left[1 - \cos(\lambda_0 t') + \frac{\lambda_0}{\lambda^*} \sin(\lambda_0 t') \right]. \quad (4.26)$$

This integral may be evaluated to yield

$$R(z) = \frac{\lambda_0^4 (\lambda^* - z)^2}{\lambda^{*2} (\lambda_0^2 + z^2)^2} (e^{-z t_p} - 1) + t_p \left[\frac{1}{z} + \frac{z(\lambda_0^2 + \lambda^{*2})}{2\lambda^{*2} (\lambda_0^2 + z^2)} \right] + 2\lambda_0^2 \cdot \frac{\lambda_0^2 + z\lambda^*}{\lambda^{*2} (\lambda_0^2 + z^2)^2} + \frac{3z}{\lambda^* (\lambda_0^2 + z^2)}. \quad (4.27)$$

In Eqs. (4.25)–(4.27) we have expressed the energy loss only in terms of the five SBB parameters. Although the final analytical expression for the energy loss is not very compact it is straightforward to evaluate it, a programmable pocket calculator suffices. Given ΔE , the rate must be evaluated by numerical integration of Eq. (3.33).

It is possible though to obtain somewhat more tractable expressions in certain limits. For $\alpha^* > 1$ one must distinguish between the weak damping limit, $\gamma^* \ll 1$, and the strong damping limit, $\gamma^* \gg 1$. For weak damping, we have already seen that our theory reduces to the well known weak damping expression for the energy loss [cf. Eqs. (3.29)–(3.31)]. The analytic result for $K(t)$ in the limit $\gamma^* \ll 1$ is:

$$K(t) \approx \frac{\gamma^*}{2} e^{-\omega^* t} (1 - \omega^* t), \quad \gamma^* \ll 1. \quad (4.28)$$

This result also holds for $\alpha^* < 1$, provided that one is truly in the weak damping limit. With this result one finds for the energy loss

$$\Delta E \approx \gamma^* V^* \left(1 + \frac{\omega^* t_p}{2} \right). \quad (4.29)$$

Using the rate expression Eq. (3.36) one recovers the weak damping result obtained by Talkner and Braun [cf. Eq. 2.41 of Ref. 17].

For the case $\gamma^* \gg \alpha^* > 1$ it has already been noted,^{3,14,15,17} that the bath is moving very sluggishly. In this limit one finds that

$$K(t) \approx \frac{\epsilon}{2} \{ \alpha^* + (\lambda^* t) [1 - (\alpha^* - 1)e^{-\lambda^* t}] - (\alpha^* - 2)e^{-\lambda^* t} \} + O(\epsilon^2) \quad (4.30)$$

showing immediately that the energy loss will be of the order of $1/\gamma^*$ as observed numerically by SBB and analysed theoretically by Talkner and Braun. The same conclusion may be obtained in terms of a sudden approximation for the bath whose details are presented in Appendix B.

The last limit to be considered is for $\alpha^* \ll 1$, but $1 \ll \gamma^*$. In this limit

$$\epsilon \approx \frac{\gamma^{*2}}{2} \gg 1 \quad (4.31)$$

and the perturbation theory in principle breaks down. Inspection of Eqs. (4.5) and (4.10) shows that in this limit, the memory friction mimics Ohmic friction. This implies that in this case one reaches a spatial diffusion limit with respect to the unstable ρ mode for which the multidimensional TST is valid. In practice, as shown in the next subsection, we find $\beta\Delta E \gg 1$ so that errors in the estimate of the energy loss are unimportant [cf. Eq. (3.33)] and the rate reduces to the multidimensional TST result.

In summary, a qualitative analysis of the theory as applied to the single well SBB problem shows that we obtain the correct qualitative behavior in all important parameter limits. The numerical results are analyzed in detail in the next subsection.

B. Numerical results

The results of the SBB simulation for the decay rate in a *double well* potential are summarized in Table I of Ref. 13(b). In this table, SBB provide numerical estimates of the rate for 36 different parameter values. The theory formulated in this paper is for a single well potential. To compare with the SBB simulation it is necessary to extract the single well rates from their numerical results. Here we note that SBB used the absorbing barrier method (ABM)^{7(e),25} to estimate the double well rates. Based on the assumptions of the ABM method, we show in Appendix C that the single well rates may be extracted from the double well rates. Denote the SBB double well transmission factor [provided in Table I of Ref. 13(b)] as f_T^{DW} . Then the single well transmission factor f_T^{SBB} is given in terms of f_T^{DW} by the expression

$$f_T^{\text{SBB}} = \frac{2f_T^{\text{DW}}(\lambda^*/\omega^*)}{f_T^{\text{DW}} + (\lambda^*/\omega^*)}. \quad (4.32)$$

The comparison presented in Fig. 1 is on a logarithmic scale. To obtain more insight into the theory we provide in Table I the same 36 parameter values, the numerical (single well) rates of SBB, and our results, for the perturbation parameter ϵ , the unstable reduced normal mode frequency (λ^*/ω^*), the reduced effective well frequency for the unstable normal mode (λ_0/ω^*), the reduced time spent in the well ($\lambda_0 t_p$), the effective normal mode barrier height (βQ^*), the energy loss ($\beta\Delta E$) and the resulting transmission coefficient f_T [cf. Eq. (3.32)].

The first six entries in Table I are for a thick barrier, corresponding to the lowest panel of Fig. 1. The physics lead-

ing to the turnover apparent in Fig. 1 are different from those of the "regular" Kramers' behavior. As is evident from Table I, here, for low and high damping the energy loss is small and the turnover is a result of slow energy diffusion in both limits. Our theory agrees very well with the simulation results. This is to be expected since for all these cases our theory is well founded (i.e., $\epsilon \ll 1$, $\beta\Delta E \ll \beta Q^*$).

Cases 7–11 correspond to the middle panel of Fig. 1. The frequency ratio $\omega^*/\omega_0 = 2$ was used to plot the piecewise parabolic potential shown in Fig. 2. For entries 7–9 we find a *large* energy loss, leading to the multidimensional TST limit and excellent agreement with the simulation, even though cases 7 and 8 are such that $\beta\Delta E > \beta Q^*$. The exponential insensitivity of the rate to the magnitude of $\beta\Delta E$ provided that $\beta\Delta E \gg 1$, is responsible for the correct result. For case 10, SBB provided results for their full reactive flux computation ($f_T^{\text{DW}} = 0.088 \pm 0.018$) and the ABM method ($f_T^{\text{DW}} = 0.126 \pm 0.024$). For the sake of consistency we use only their ABM result although the full reactive flux computation does give much better agreement. The discrepancy between their two numbers implies that the typical error in the numerical results is $\sim 50\%$, i.e., somewhat larger than the statistical estimates of SBB.

Entries 14–20 are for a thin barrier. As already shown in the top panel of Fig. 1, good agreement is found in the weak damping limit. In the intermediate and strong damping range (17–19), there seems to be a discrepancy. For these entries we find an energy loss that is *greater* than the normal mode barrier height (βQ^*). For case 20 the energy loss is only somewhat smaller than βQ^* . This means that the estimate of $\beta\Delta E$ is not very accurate. Since here the energy loss is not large, the inaccuracy in $\beta\Delta E$ will reflect itself in the estimate for the rate.

We have stressed the fact that the turnover shown in Fig. 1 is a result of slow energy diffusion in both weak and strong damping limits. To gain more insight, we plot in Fig. 3 the bath function $K(t)$ [cf. Eq. (4.24)] whose behavior

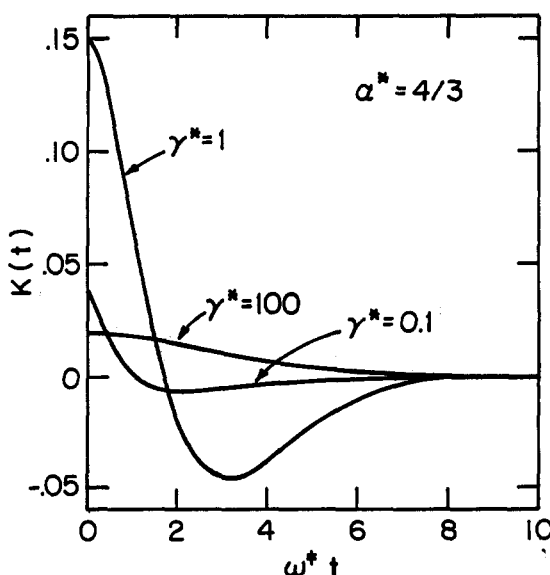


FIG. 3. The function $K(t)$ for exponential memory friction [cf. Eq. (4.24)]. The function is shown for $\alpha^* > 1$, such that in the weak and strong damping limits, energy diffusion is slow.

TABLE I. Theoretical parameters and transmission coefficients for the SBB system.

No.	BV^*	ω^*/ω_0	γ^*	α^*	λ^*/ω^*	λ_0/ω^*	$\lambda_0 t_p$	ϵ	BQ^*	$B\Delta E$	f_T	f_T^{SBBa}
1	20	0.2	0.01	4/3	0.995 1	4.988	3.535	4.89(−3)	19.90	0.539 5	0.294	0.299 ± 0.039
2	20	0.2	0.1	4/3	0.956 6	4.905	3.527	0.041 11	19.02	4.866	0.836	0.843 ± 0.055
3	20	0.2	1	4/3	0.785 1	4.685	3.474	0.152 0	14.04	13.98	0.779	0.765 ± 0.073
4	20	0.2	10	4/3	0.579 6	5.798	3.382	0.113 2	7.297	4.812	0.505	0.500 ± 0.052
5	20	0.2	100	4/3	0.510 7	5.022	3.344	0.020 50	5.172	0.583 7	0.160	0.171 ± 0.029
6	20	0.2	1000	4/3	0.501 1	5.069	3.339	2.23(−3)	4.887	0.059 43	0.024 3	0.020 ± 0.010
7	20	2	0.1	4/3	0.956 6	0.534 3	5.264	0.041 11	16.03	17.22	0.953	0.955 ± 0.042
8	20	2	1	4/3	0.785 1	0.684 6	4.849	0.152 0	6.577	31.45	0.785	0.782 ± 0.071
9	20	2	10	4/3	0.579 6	0.887 1	4.299	0.113 2	2.134	5.939	0.528	0.557 ± 0.075
10	20	2	100	4/3	0.510 7	0.981 9	4.101	0.020 50	1.353	0.528 2	0.149	0.202 ± 0.046
11	20	2	1000	4/3	0.501 1	0.998 0	4.072	2.23(−3)	1.261	0.051 33	0.021 3	0.035 ± 0.008
12	100	2	1000	4/3	0.501 1	0.998 0	4.072	2.23(−3)	6.303	0.256 7	0.084 8	0.114 ± 0.016
13	1000	2	1000	4/3	0.501 1	0.998 0	4.072	2.23(−3)	63.03	2.567	0.357	0.432 ± 0.034
14	20	20	0.0001	4/3	0.999 95	0.050 50	6.182	5.00(−5)	19.61	0.2439	0.163	0.225 ± 0.034
15	20	20	0.001	4/3	0.999 5	0.054 76	6.174	4.99(−4)	16.66	1.909	0.627	0.709 ± 0.059
16	20	20	0.01	4/3	0.995 1	0.086 24	6.110	4.89(−3)	6.656	4.779	0.865	0.994 ± 0.021
17	20	20	0.1	4/3	0.956 6	0.218 5	5.834	0.041 11	0.958 1	2.423	0.666	0.976 ± 0.016
18	20	20	1	4/3	0.785 1	0.503 8	5.142	0.152 0	0.121 4	0.764 3	0.294	0.499 ± 0.076
19	20	20	10	4/3	0.579 6	0.751 4	4.456	0.113 2	0.029 75	0.106 8	0.047 3	0.102 ± 0.012
20	20	20	100	4/3	0.510 7	0.849 4	4.224	0.020 50	0.018 08	0.008 774	0.004 15	0.012 ± 0.004
21	20	2	1	0.001	0.618 2	0.556 1	4.818	0.807 8	6.179	27.94	0.618	0.614 ± 0.053
22	20	2	10	0.001	0.099 12	0.1205	4.518	50.35	3.383	18.96	0.0989	0.102 ± 0.022
23	20	20	10	0.01	0.099 99	0.1002	4.710	49.02	0.049 77	0.2843	0.018 3	0.053 ± 0.017
24	20	20	0.1	0.01	0.951 3	0.218 1	5.832	0.052 46	0.951 2	2.384	0.658	0.940 ± 0.065
25	20	0.2	100	0.1	0.011 11	0.083 7	3.406	3.64(+3)	8.808	124.0	0.0111	0.012 ± 0.012
26	20	0.2	100	0.5	0.019 98	0.202 7	3.338	626.0	4.862	100.4	0.0200	0.029 ± 0.019
27	20	2	300	0.5	0.006 666	0.013 33	4.069	5.63(+3)	1.250	7.613	0.006 31	0.009 ± 0.009
28	20	0.2	100	0.7	0.033 2	0.434 1	3.294	136.2	2.927	622.0	0.33 2	0.051 ± 0.024
29	20	0.2	300	1	0.148 3	4.17 6	3.313	0.489 0	0.6304	1.378	0.079 0	0.074 ± 0.036
30	20	2	100	2.5	0.775 9	0.803 6	4.677	1.69(−3)	4.661	0.459 4	0.205	0.220 ± 0.061
31	20	2	1000	2.5	0.774 7	0.806 0	4.673	1.72(−4)	4.620	0.045 99	0.029 9	0.048 ± 0.020
32	20	2	300	10	0.948 7	0.591 6	5.168	1.95(−5)	12.86	0.049 11	0.038 8	0.047 ± 0.028
33	20	0.2	0.1	25	0.985 7	4.992	3.531	4.23(−3)	19.49	0.602 4	0.315	0.233 ± 0.035
34	20	0.2	1	25	0.980 6	5.002	3.529	7.84(−4)	19.22	0.111 0	0.082 8	0.043 ± 0.014
35	20	20	10	25	0.979 9	0.205 6	5.870	8.43(−5)	1.136	0.389 2	0.229	0.247 ± 0.065
36	20	20	100	25	0.979 8	0.206 1	5.869	8.50(−6)	1.130	0.039 91	0.033 2	0.031 ± 0.012

^a These are the numerical results of the SBB simulation, cf. Table I of Ref. 13(b).

really determines the energy loss. For weak damping, ($\gamma^* = 0.1$) $K(t)$ is well approximated by Eq. (4.28). The function shows a rapid exponential falloff, the magnitude is small, leading to a small energy loss. As the damping increases, ($\gamma^* = 1$) the falloff becomes slower, the magnitude increases and so does the energy loss, leading to the multidimensional TST limit. For strong damping, the falloff becomes very slow, as already mentioned (cf. Appendix B), the bath becomes very sluggish, justifying a sudden approximation. The magnitude of $K(t)$ also decreases, all this leads to very small energy loss, and an energy diffusion limited rate.

Entries 21, 22, and 25–28 all correspond to the multidimensional TST limit. Here, $\alpha^* < 1$, at high damping the energy loss becomes large, full equilibration is achieved, and f_T is given simply by the Grote–Hynes factor, as also noted by Talkner and Braun.¹⁷ In all these cases, the perturbation parameter ϵ is not small, leading to large energy loss and the correct multidimensional TST limit. Discrepancies found in entries 26–28 *must* be errors in the numerical simulation since the Grote–Hynes factor (λ^*/ω^*) is an upper bound for the transmission factor f_T . Talkner and Braun reach the same conclusion.

It is interesting to note that for $\alpha^* < 1$, $\gamma^* \gg 1$ the function $K(t)$ differs qualitatively from the sudden limit. This is shown in Fig. 4. Although for $\gamma^* \gg 1$ there is an overall slow decay, it is modulated by a rapid oscillation. Analysis of Eqs. (4.21)–(4.24) shows that in this limit ($\alpha^* \ll 1, \alpha^* \gamma^* \gg 1$)

$$K(t) \approx \epsilon \exp\left(-\frac{\omega^* t}{2\alpha^* \gamma^*}\right) \cos\left(\frac{\omega^* t}{\sqrt{\alpha^*}}\right). \quad (4.33)$$

For $\alpha^* < 1$ and large damping, there is only one dominant term with high frequency ($\omega^*/\sqrt{\alpha^*}$) that contributes to $K(t)$. Since the discretized form of $K(t)$ is a weighted sum of cosine functions [cf. Eq. (2.22)], one may conclude from Eq. (4.32) that in the limit $\gamma^* \rightarrow \infty$, the dynamics reduce to those of a two degree of freedom system where the bath oscillator has a high frequency ($\omega^*/\sqrt{\alpha^*}$). Since $\epsilon \gg 1$ we have $u_{00} \ll 1$ [cf. Eq. (2.20)] and the unstable normal mode is almost perpendicular to the system coordinate q , which because there are only two degrees of freedom, must now coin-

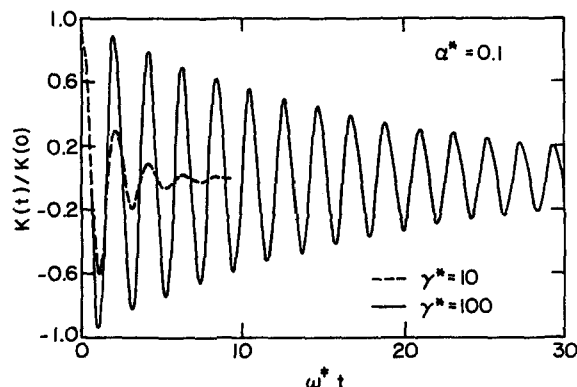


FIG. 4. The function $K(t)$ in the spatial diffusion limit, $\alpha^* < 1$, $\alpha^* \gamma^* > 1$. Note that $K(0) = 37.04, 3646$ for $\gamma^* = 10, 100$, respectively.

cide with the bath model! One thus expects for short times, that the motion along the q coordinate will be almost harmonic. The dynamics are such that the unstable normal mode motion is very slow in comparison to the bath. Because of the large damping, this leads to a large energy transfer and so the multidimensional TST limit is obtained. Because of the very slow motion of the unstable normal mode, a time average over the system coordinate will show for long times a slow diffusive motion as seen in Fig. 4(b) of SBB [ref. 13(b)]. In this limit the term spatial diffusion is justified. The turnover in the rate as one goes from weak to strong damping is here, identical in nature to the original Kramers turnover. Some typical examples are shown in Fig. 5.

Entry 23 is especially interesting. The perturbation parameter $\epsilon \gg 1$ and the energy loss $\beta \Delta E > \beta Q^*$. However, the energy loss is quite small. In this case our theory should fail and in fact we find at least a factor of two difference. Likewise, entries 24 and 29 correspond to a possible inaccuracy of our theory, similar to entries 17–19 (although for 29 agreement is actually very good). In these cases $\epsilon < 1$ and the energy loss is greater than the barrier height.

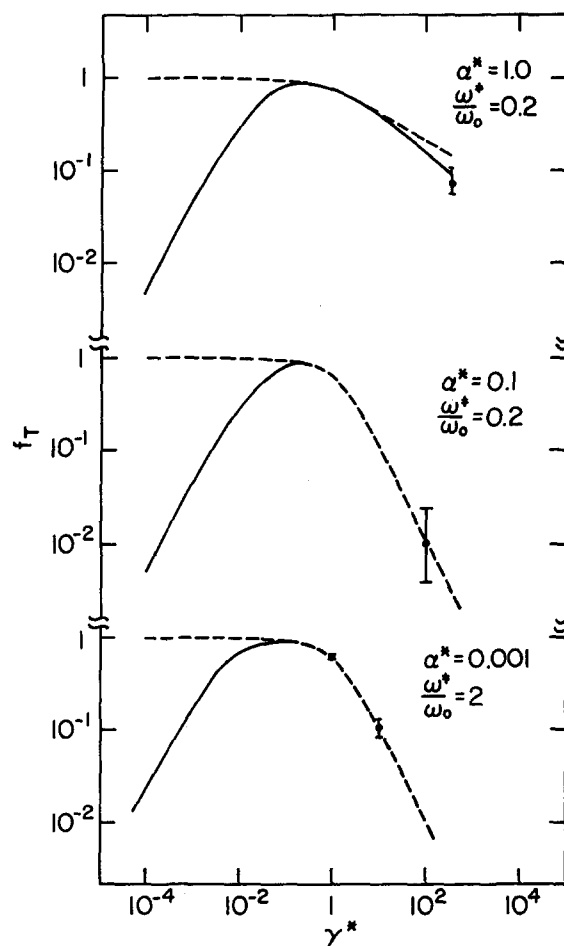


FIG. 5. Turnover from energy diffusion to spatial diffusion limited escape. The solid lines are based on the present theory, dashed lines are the multidimensional TST [Eq. (3.8)], filled circles with bars are from the SBB single well simulation results, cf. Table I. For large γ^* , when the dashed line coincides with the solid line, only the former is shown. Note that for $\alpha^* = 1$ at large damping there is already a substantial deviation from the multidimensional TST. Here, the rate again becomes energy diffusion limited.

Entries 30–36 all deal with $\alpha^* \gg 1$ and $\epsilon \leq 1$, these are limits when theory should be good. Thus discrepancies in entries 33 and 34 are probably due to inaccuracy in the numerical simulation.

In summary, our theory agrees with *all* SBB data within a factor of two. Considering the numerical uncertainties in the simulation and the few cases where we identify a breakdown in conditions for validity of our theory, we believe that this agreement may be considered as satisfactory.

V. DISCUSSION

The turnover theory presented in Sec. III is quite general. Starting from a GLE we obtain expressions which are uniquely determined by the system potential, $V(q)$ and the memory friction, $\gamma(t)$. In this sense the theory has been formulated for arbitrary friction.

Our analysis of the SBB system has highlighted the fact that there are two very different mechanisms that can lead to a turnover of the rate of escape as a function of the damping strength. The usual transition from energy diffusion at low damping to spatial diffusion at large damping is found in the SBB system when the parameter $\alpha^* < 1$. This limit is characterized by small energy loss from the unstable normal mode at weak damping but very large energy loss at large damping, leading to an equilibrium energy distribution and the validity of multidimensional TST. Some graphical examples of this turnover (based on our theory) are presented in Fig. 5. The second turnover mechanism is one for which the rate is limited by energy diffusion in both weak and high damping limits. This is the case when the SBB parameter $\alpha^* > 1$, examples of this turnover are shown in Fig. 1. This mechanism is characterized by small energy loss in both limits. Our theory describes correctly both mechanisms without any ad hoc assumptions or any adjustable parameters.

The formal generality of the theory does not imply that it is always valid. For example, if the spectral density has a very narrow peak around some frequency, one would expect this frequency region to be strongly coupled to the unstable normal mode leading to two relatively large normal mode transformation matrix elements. In this case, the perturbation parameter ϵ will be of order one, and one would expect that the perturbative solution of the equations of motion will no longer be valid.

On a simpler level, we have seen that for Ohmic dissipation, in the strong damping limit, $\epsilon \gg 1$. In this case though, exponential insensitivity of the rate to the magnitude of the energy loss ΔE , when $\beta \Delta E \gg 1$ [cf. Eq. (3.33)] still leaves us with a theory that reduces to the correct multidimensional TST limit. In fact, when $\epsilon \gg 1$ the theory predicts a large energy loss which implies fast thermalization and validity of multidimensional TST. Thus the theory extends correctly also to cases when $\epsilon > 1$. Explicit examples are found in the SBB simulation. However, when $J(\omega)$ has a narrow peak around one or more frequencies one might expect a selective energy mixing which would not allow rapid thermalization and in this limit the theory as it stands would break down. For example, in realistic models,²⁶ the energy loss shows irregular behavior near the barrier region and cannot be assumed to be a constant in a region of width $k_B T$. Such a

breakdown would be the dissipative counterpart to what is known as non-RRKM behavior in gas phase chemistry.¹⁴ In principle such a situation could be remedied by explicit solution for the simultaneous equations of motion of the unstable and strongly coupled mode. This is though beyond the scope of the present paper.

The theory presented in this paper is for a single well potential. Generalization to an asymmetric double well potential is straightforward, all one needs to do is to adapt Melnikov and Meshkov's⁹ Eq. (8.8) to the unstable mode dynamics in both wells.

Perhaps the most important result of this paper is that in classical mechanics, the motion along the unstable normal mode really determines the escape dynamics. The same is true in quantum mechanics as demonstrated for example in Refs. 19 and 27. Briefly, since $\lambda \neq \omega^*$, the normal mode barrier is thicker as a result of dissipation, leading to an exponential decrease of tunneling rates. Elsewhere, the present approach will be generalized to treat the case of quantal escape dynamics.

ACKNOWLEDGMENTS

We thank Professor B. J. Berne and Dr. I. Rips for stimulating discussions. H. G. thanks the Department of Chemistry, Columbia University, N.Y. for their kind hospitality during an extended stay. This work has been supported by grants of the Minerva Foundation, the U. S.—Israel Binational Science Foundation, the Deutsche Forschungsgemeinschaft, through Sonderforschungsbereich 237, and the Albert Leimar Foundation.

APPENDIX A: RESPONSE FUNCTION IN THE BARRIER REGION

Let us consider the response of the system coordinate to an external driving force $f(t)$ when the system moves in the barrier region where the potential may be approximated by Eq. (2.5). From Eq. (1.1) the deterministic equation of motion for the reaction coordinate reads

$$\ddot{q}(t) - \omega^* q(t) + \int_0^t dt' \gamma(t-t') \dot{q}(t') = f(t)/M. \quad (A1)$$

The response of $q(t)$ to the force $f(t)$ is described in terms of a response function $\Xi(t)$ the Laplace transform of which reads

$$\hat{\Xi}(s) = [s^2 + s\hat{\gamma}(s) - \omega^*]^{-1}. \quad (A2)$$

On the other hand, using the normal mode representation Eq. (2.13) and the Hamiltonian (2.9), we find

$$\hat{\Xi}(s) = \frac{u_{00}^2}{s^2 - \lambda^*{}^2} + \sum_{j=1}^N \frac{u_{j0}^2}{s^2 + \lambda_j^2} \quad (A3)$$

This representation reveals the divergent part of the response arising from the instability of an inverted parabolic potential. Hence, the regular part of the response function, which decays in the time domain, is given by

$$\begin{aligned} \text{Reg}[\hat{\Xi}(s)] &= \sum_{j=1}^N \frac{u_{j0}^2}{s^2 + \lambda_j^2} \\ &= [s^2 + s\hat{\gamma}(s) - \omega^{\neq 2}]^{-1} - \frac{u_{00}^2}{s^2 - \lambda^{\neq 2}}. \quad (\text{A4}) \end{aligned}$$

Now, apart from a factor $1/u_{00}^2$, the first expression on the right-hand side is just the Laplace transform of $K(t)$ [cf. Eq. (2.22)], and we immediately obtain Eq. (2.23).

APPENDIX B: SUDDEN APPROXIMATION FOR THE CASE $\alpha^*\gamma^* \gg 1$

For the exponential friction used in the SBB problem one finds that the spectral density $J(\omega)$ is given by [cf. Eq. (2.4)]

$$J(\omega) = \omega\omega^{\neq} \frac{\gamma^*}{1 + (\omega/\omega^{\neq})^2 \alpha^* \gamma^*}. \quad (\text{B1})$$

For frequencies $\omega \gg \omega^{\neq}/\alpha^*\gamma^*$ this implies that

$$J(\omega) \sim \frac{\omega^{\neq 3}}{\omega \alpha^* \gamma^*} \quad (\text{B2})$$

therefore in the limit that $\alpha^*\gamma^* \gg 1$ the spectral density has contributions from only very low frequency modes. This is a quantitative expression for the sluggishness of the bath modes. In this Appendix we use this observation to derive an expression for the energy loss, in this limit. Combining Eqs. (2.22), (3.28), (4.19), and (4.20) one finds by direct integration

$$\begin{aligned} \Delta E &= 4V^{\neq} (\lambda_0^2 + \lambda^{\neq 2}) \lambda^{\neq 4} \frac{\omega_0^2}{\omega^{\neq 2}} \sum_{j=1}^N \frac{u_{j0}^2}{\lambda_j^2} \\ &\times \frac{[\sin(\lambda_j t_p/2) + (\lambda_j/\lambda^{\neq}) \cos(\lambda_j t_p/2)]^2}{(\lambda_j^2 - \lambda_0^2)^2}. \quad (\text{B3}) \end{aligned}$$

The time $t_p \sim 1/\lambda_0$ and all bath frequencies are very small so that $\lambda_j t_p \ll 1$. We may therefore expand the expression to first order in $(\lambda_j/\lambda_0)^2$. This gives the simple result

$$\begin{aligned} \Delta E &\approx \left(\sum_{j=1}^N u_{j0}^2 \right) \cdot V^{\neq} \frac{(\lambda_0^2 + \lambda^{\neq 2})}{\lambda_0^2} \frac{\lambda^{\neq 4}}{\lambda_0^4} \frac{\omega_0^2}{\omega^{\neq 2}} \\ &\times \left(\lambda_0 t_p + 2 \frac{\lambda_0}{\lambda^{\neq}} \right)^2. \quad (\text{B4}) \end{aligned}$$

Since $\sum_{j=1}^N u_{j0}^2 = \epsilon/(1 + \epsilon)$, and $\epsilon \ll 1$ we find to first order in the perturbation parameter ϵ that the energy loss is

$$\Delta E \approx \epsilon Q^{\neq} \frac{\lambda^{\neq 2}}{\lambda_0^2} \left(1 + \frac{\lambda^{\neq 2}}{\lambda_0^2} \right) \left(\lambda_0 t_p + 2 \frac{\lambda_0}{\lambda^{\neq}} \right)^2 + O(\epsilon^2). \quad (\text{B5})$$

APPENDIX C: SINGLE WELL RATES OF THE SBB SIMULATION

As noted in Sec. IV, SBB present numerical results for the decay rate in a symmetric (piecewise parabolic) double well potential based on the ABM.^{7(e),25} In this Appendix we show how their results may be inverted to obtain the single well rate. It should be stressed though that this inversion is correct provided that the statistical independence assumption underlying the ABM method is valid.

As noted by Straub and Berne,^{7(e)} the reactive flux, in a double well potential, with a high barrier ($\beta V^{\neq} \gg 1$) will decay exponentially at long times

$$k(t) \sim \lambda_{\text{plat}} e^{-(k_f + k_b)t}, \quad (\text{C1})$$

where k_f and k_b are the forward and backward rate constants and λ_{plat} is the "plateau value" of the reactive flux

$$\lambda_{\text{plat}} = \frac{k_f + k_b}{(k_f + k_b)_{\text{TST}}}. \quad (\text{C2})$$

The assumption of statistical independence of consecutive recrossings of the transition state (TS) leads to the fundamental relation of the ABM [Eq. (10) of Ref. 7(e)]

$$\lambda_{\text{plat}} = \frac{T_A T_B}{T_A + T_B - T_A T_B}, \quad (\text{C3})$$

where T_A (T_B) is defined as the fraction of trajectories integrated along the system coordinate q that originate at the TS with velocity in direction of well A (B) which immediately get trapped in A (B) and so do not quickly recross the barrier.

The numerical simulation results of SBB for the symmetric double well potential denoted here as f_T^{DW} are identical to λ_{plat} . It follows from Eq. (C3) that ($T_A = T_B \equiv T_0$)

$$T_0 = \frac{2f_T^{\text{DW}}}{1 + f_T^{\text{DW}}}. \quad (\text{C4})$$

Similarly, for a purely harmonic barrier, the rate is exactly the multidimensional TST limit [Eq. (3.8)] so that $\lambda_{\text{plat}} = \lambda^{\neq}/\omega^{\neq}$. This implies that for the pure barrier with $T_A = T_B \equiv T^{\neq}$, the fraction that immediately gets trapped when integrating along the system coordinate q is

$$T^{\neq} = \frac{2\lambda^{\neq}/\omega^{\neq}}{1 + \lambda^{\neq}/\omega^{\neq}}. \quad (\text{C5})$$

For the single well problem, the assumption of statistical independence of recrossings allows us to estimate T_A which is the fraction that immediately gets trapped in the well, from the symmetric double well result so that $T_A = T_0$. On the other hand, T_B , the fraction that crosses the barrier and doesn't return (because there is no well in the B region) is obtained from the pure barrier case, that is $T_B = T^{\neq}$. Inserting this with Eqs. (C4) and (C5) into Eq. (C3) leads to the desired result [cf. Eq. (4.32)]

$$f_T^{\text{SBB}} = \frac{2f_T^{\text{DW}}(\lambda^{\neq}/\omega^{\neq})}{f_T^{\text{DW}} + \lambda^{\neq}/\omega^{\neq}}. \quad (\text{C6})$$

Since f_T^{DW} is given by SBB with error bounds, one can estimate from this result new error bounds on f_T^{SBB} in standard fashion. The single well estimate f_T^{SBB} with its error bounds are given in Table I.

¹H. A. Kramers, *Physica* **7**, 284 (1940).

²J. T. Hynes, in *Theory of Chemical Reaction Dynamics*, edited by M. Baer (CRC, Boca Raton, 1985) Vol. IV, p. 171.

³P. Hänggi, *J. Stat. Phys.* **42**, 105 (1986).

⁴B. J. Berne, M. Borkovec, and J. E. Straub, *J. Phys. Chem.* **92**, 3711 (1988).

⁵A. Nitzan, *Adv. Chem. Phys.* **70**, 489 (1988).

⁶J. Troe, in *Physical Chemistry—An Advanced Treatise*, edited by W. Jost (Academic, New York, 1975) Vol. VIB, p. 835.

- ⁷P. Hänggi and U. Weiss, *Phys. Rev. A* **29**, 2265 (1984); B. Carmeli and A. Nitzan, *Phys. Rev. A* **29**, 1481 (1984); B. J. Matkowsky, Z. Schuss, and C. Tier, *J. Stat. Phys.* **35**, 443 (1984); A. G. Zawadski and J. T. Hynes, *Chem. Phys. Lett.* **113**, 476 (1985); J. E. Straub and B. J. Berne, *J. Chem. Phys.* **83**, 1138 (1985); J. A. M. Janssen, *Physica A* **152**, 145 (1988).
- ⁸J. L. Skinner and P. G. Wolynes, *J. Chem. Phys.* **72**, 4913 (1980); B. Cartling, *J. Chem. Phys.* **87**, 2638 (1987).
- ⁹V. I. Melnikov and S. V. Meshkov, *J. Chem. Phys.* **85**, 1018 (1986).
- ¹⁰R. F. Grote and J. T. Hynes, *J. Chem. Phys.* **73**, 2715 (1980).
- ¹¹P. Hänggi and F. Mojtabai, *Phys. Rev. A* **26**, 1168 (1982).
- ¹²B. Carmeli and A. Nitzan, *Phys. Rev. Lett.* **49**, 423 (1982).
- ¹³J. E. Straub, M. Borkovec, and B. J. Berne, *J. Chem. Phys.* **83**, 3172 (1985); *ibid.* **84**, 1788 (1986).
- ¹⁴J. E. Straub and B. J. Berne, *J. Chem. Phys.* **85**, 2999 (1986).
- ¹⁵R. Zwanzig, *J. Chem. Phys.* **86**, 5801 (1987).
- ¹⁶S. Okuyama and D. W. Oxtoby, *J. Chem. Phys.* **84**, 5830 (1986).
- ¹⁷P. Talkner and H. B. Braun, *J. Chem. Phys.* **88**, 7537 (1988).
- ¹⁸H. Grabert, *Phys. Rev. Lett.* **61**, 1683 (1988).
- ¹⁹E. Pollak, *J. Chem. Phys.* **85**, 865 (1986); *Phys. Rev. A* **33**, 4244 (1986).
- ²⁰A. M. Levine, M. Shapiro, and E. Pollak, *J. Chem. Phys.* **88**, 1959 (1988).
- ²¹A. M. Levine, W. Hontscha, and E. Pollak, *Phys. Rev. B* **40**, 2138 (1989); E. Pollak, *Israel J. Chem.* (in press).
- ²²R. Zwanzig, *J. Stat. Phys.* **9**, 215 (1973).
- ²³R. Zwanzig, *Phys. Fluids* **2**, 12 (1959).
- ²⁴See e.g., H. Hochstadt, *Integral Equations* (Wiley, New York, 1973).
- ²⁵J. E. Straub, D. A. Hsu, and B. J. Berne, *J. Phys. Chem.* **89**, 5188 (1985).
- ²⁶H. Grabert and S. Linkwitz, *Phys. Rev. A* **37**, 963 (1988).
- ²⁷W. Hontscha and P. Hänggi, *Phys. Rev. A* **36**, 2359 (1987).